buildings

MDPI

Article

Parametric Study of Lightweight Wooden Wall Assemblies for Cold and Subarctic Climates Using External Insulation

Alexis Caron-Rousseau [1], Pierre Blanchet [1,*] and Louis Gosselin [2]

[1] Department of Wood and Forest Sciences, Université Laval, Quebec City, QC G1V 0A6, Canada; alexis.caron-rousseau.1@ulaval.ca
[2] Department of Mechanical Engineering, Université Laval, Quebec City, QC G1V 0A6, Canada; louis.gosselin@gmc.ulaval.ca
* Correspondence: pierre.blanchet@sbf.ulaval.ca

Abstract: While externally insulated wall assemblies are widely recognized for their hygrothermal performance, few research projects have focused on the impact of shifting the entire wall insulation to the exterior side of a structural cavity in cold or subarctic climates or its effectiveness in terms of acoustic performance and airtightness. The objective of this study was to propose fully externally insulated assemblies that could be used in cold and subarctic climates by assessing the benefits of the hygrothermal performance of these assemblies and by achieving a comparable airtightness and sound transmission performance to the modern assemblies that are currently built in North America. The results suggested that the externally insulated assemblies limited the risk of condensation occurring inside structural cavities and allowed for faster drying than the modern assemblies when exposed to water infiltration or high water contents in all climates that were tested. The assemblies with external airtight insulation boards were more airtight than assemblies with air barrier membranes and, in addition, assemblies with external soundproof insulation were shown to be necessary to achieve a comparable sound transmission loss to that of a modern assembly.

Keywords: thermal resistance; wall partitions; building envelope; airtightness; transmission loss; noise insulation; hygrothermal simulation; airflow; building; mold index

Citation: Caron-Rousseau, A.; Blanchet, P.; Gosselin, L. Parametric Study of Lightweight Wooden Wall Assemblies for Cold and Subarctic Climates Using External Insulation. *Buildings* **2022**, *12*, 1031. https://doi.org/10.3390/buildings12071031

Academic Editors: John Gardner, Seongjin Lee, Kee Han Kim and Sukjoon Oh

Received: 8 May 2022
Accepted: 8 July 2022
Published: 17 July 2022

1. Introduction

The building sector is the second most energy-hungry sector in the world after transportation, consuming 33% of the global energy that is produced annually [1]. Regulations that have been implemented by various governments have helped to reduce the sector's energy consumption [2]. In Canada, the residential and commercial sectors accounted for 16.6% and 11.4% of the total secondary energy use in 2016, respectively. The cooling and heating needs of residential houses and apartments represent 63% of the total energy use of those buildings [3]. Increasing the energy efficiency of residential buildings directly contributes to reducing their cooling and heating loads and, in turn, their energy consumption.

Energy efficiency policies, standards and codes for buildings have become more and more strict over the years. For example, Chapter B-1.1 of the Quebec Construction Code (QCC), which came into effect in 2020, takes a new approach to building energy efficiency. It sets out effective thermal resistance values that are more stringent than the total thermal resistance values that were proposed in previous editions of the code. QCC also regulates the energy efficiency of houses and small buildings, which also requires higher thermal resistance values than the previous versions of the QCC [4,5].

The building envelope is one of the main building systems that influence energy consumption. A properly designed building envelope can reduce energy consumption [6–8], maintenance costs [9] and greenhouse gas emissions [10–12], as well as increasing occupant comfort [9,13]. However, the building envelope is a part of the exterior envelope and,

therefore, is a truly multifunctional system. The complexity that is created by building envelopes having multiple required features can keep the industry from altering designs and construction methods because a change to one component of the envelope could negatively influence other assembly functions [14,15].

The industry is known to be slow to adopt the results of building science research, which has been attributed in the literature to a learning-by-doing process [16], a lack of knowledge transfer [17], a lack of holistic approaches to envelope design [16,18] and a failure to adapt to the environment in which the envelope is built [19], among other reasons.

One potential solution for improving envelope performance is to use external insulation. This approach was first developed by Hutcheon [20] and was more recently described in Lstiburek's article [21] on the so-called "perfect wall" (see Figure 1). Externally insulated walls work in every climate. In subarctic regions, the structural cavities of walls must remain uninsulated to limit the condensation of cold air. In the external insulation approach, the various layers of the building envelope, such as the air control layer, vapor control layer and thermal control layer, are installed on the outside of a light-frame construction to protect the structural layer, reduce thermal bridging and condensation risks and improve the performance of the thermal insulation [21].

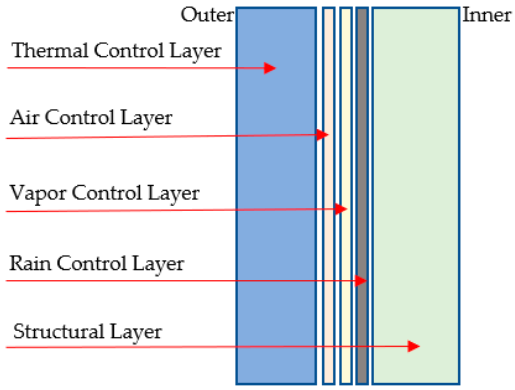

Figure 1. A schematic representation of the control layers and their positions, according to Lstiburek's "perfect wall" concept. Externally insulated assemblies have been studied for their ability to reduce the thermal bridging that is caused by the repetition of structural elements, such as studs, in light-frame constructions and to reduce the risk of condensation inside structural cavities, specifically on the backside of the sheathing.

Lstiburek's external insulation approach [21] is illustrated in Figure 1. It proposes that when the thermal control layer is positioned outside of the structural layer, it helps to prevent moisture buildup from condensation, water infiltration and the expansion of wood studs due to temperature changes in the structural layer. Separating the structural layer from the external air, which can carry moisture and impact the sheathing temperature, helps to limit the risk of condensation in the assembly. Positioning the air barrier under the thermal control layer prevents external air from infiltrating the structural layer and reaching its dew point within that layer. Positioning the vapor barrier and rain control layer between the thermal insulation and the structural layer reduces the risk of condensation diffusing into the thermal layer and helps it to drain externally when flashing is installed at the base of the membrane and at the openings in the building envelope [21,22].

Straube and Smegal [23] compared the thermal resistance of various insulation methods that are used in North America. They found that in most cases, the measured R-values were less than the theoretical values and demonstrated that most walls that had R-values approaching 20 performed poorly in cold climates. In addition, all walls with R-values above 30 could reduce thermal bridging. They found that adding external insulation to a structure had several advantages in terms of durability and energy efficiency. They also studied 17 typical assemblies that are used in Western Canada [24] and found that most assemblies with insulation that was outside of the cavities had limited numbers of hours

during which they were at risk of cavity condensation from air infiltration. The external insulation made it possible to keep the external surface of a cavity warmer, thereby limiting the number of hours during which it was below the dew point. Again, the assemblies with the best performances had thermal insulation on the outside of the cavities.

More recently, Trainor [25] expanded on Straube and Smegal's research by studying externally insulated assemblies according to the type of insulation that was used. They compared an extruded polystyrene (XPS) board, a mineral wool board and a polyisocyanurate board, all of which were used on the outside of structural cavities, as well as a double stud assembly that was filled with dense cellulose and a traditional wall without external insulation. The walls were evaluated for thermal and moisture performance under air injection conditions and when wetting mats were incorporated into the assemblies.

Their results suggested that only the double stud wall was vulnerable to winter condensation. In addition, all of the externally insulated walls showed lower risks of air penetration than the other assemblies that were tested. During the wetting phase, the polyisocyanurate and XPS assemblies were significantly less able to dry from the exterior and while the mineral wool wall was also less able to dry from the exterior, it was more able than the other two assemblies. As for the conventional and double stud walls, they were sufficiently able to dry from the outside. This work concluded that the addition of insulation to the exterior side of a wall was beneficial for limiting the risk of air infiltrating the assembly. In addition, the results suggested that the amount of external insulation needed to be adapted to the climate and interior humidity level. Finally, the insulation materials that were placed on the outside of the cavities slowed the drying of the assembly from the exterior and, therefore, their use could be of interest in areas where water vapor diffusion from the exterior is possible or the drying of an assembly from the interior is assured.

Craven and Garber-Slaght [26] studied the potential for condensation to cause moisture accumulation in wall assemblies in subarctic climates. Their results indicated that the assemblies with the most external insulation had the lowest relative humidity (RH) inside the sheathing. Walls with external insulation and interior vapor barriers showed similar results but responded more slowly, requiring several months to reduce the RH after reaching a maximum RH in winter. In walls with polyethylene vapor barriers, mold was visible where there were unsealed penetrations, such as electrical boxes. The article concluded that the ratio of external to internal insulation had a greater impact on hygrothermal performance than the use of polyethylene.

Ge and Straube's study indicated that an increase in the moisture content of the OSBs in externally insulated assemblies was lower than that in deep cavity assemblies (double stud walls, I-joist walls and spray foam walls) when air war injected into the walls. They also indicated that the increase in the OSB moisture content depended on the type of external insulation that was used as XPS and mineral wool caused smaller increases [27].

While the addition of cavity insulation, air sealing, airspace and high mass are well-known practices for improving the acoustical performance of assemblies [28,29], very few studies have investigated the acoustical performance of insulated assemblies and the impact of the ratio of external to internal cavity insulation on sound transmission. The studies that we consulted instead dealt with the acoustic and thermal performance of materials [30,31], the impact of interior wall covering on sound transmission [32,33] or the addition of draining cavities behind external cladding [34].

Despite these advances, there are still several challenges to be addressed regarding the external insulation of residential building envelopes. The ratio between the amount of external insulation and cavity insulation and its impact on the hygrothermal behavior and airtightness of the assemblies have been extensively studied in the literature. However, fully externally insulated assemblies that provide adequate hygrothermal performance for lightweight wooden wall assemblies in cold and subarctic climates have not been investigated in the above-mentioned studies. Furthermore, the impact of shifting thermal insulation and vapor barriers to the exterior of structural cavities, as well as shifting air

barrier layers to underneath the thermal insulation, on the acoustical transmission loss and airtightness of assemblies has not yet been investigated.

The objective of this study was to propose fully externally insulated assemblies that could be used in cold and subarctic climates by assessing the benefits of the hygrothermal performance of these assemblies and by achieving a comparable airtightness and sound transmission performance to the modern assemblies that are currently built in North America. This study combined laboratory tests with hygrothermal simulations.

2. Materials and Methods

The performance of externally insulated assemblies was compared to that of a modern assembly that was largely considered to be energy efficient as it contained more thermal insulation than is required by the National Building Code of Canada (NBC). This latter assembly consisted of a fully insulated 38 mm × 140 mm frame that was sheathed with oriented strand board that was 11 mm thick and rigid insulation foam that was 38 mm thick, which were fixed to the exterior of the frame.

This section describes the tests that were performed to measure the airtightness and airborne sound transmission loss of the wall specimens, as well as the relative humidity and temperature inside the wall specimens. The probes and equipment that were used to perform these measurements are also presented. The externally insulated assemblies were optimized according to the results from the previous specimen to reach the values that are required by the codes and to exceed the values of the light-frame assembly with cavity insulation. The choice of materials that were used to build the next specimen was made in accordance with this analysis. WUFI® hygrothermal simulations were performed to measure the hygrothermal performance and the risk of mold growth in cold and subarctic climate zones. The water content, as well as the mold growth index (which was developed by Hukka and Viitanen [35] and was also more recently enhanced by Ojanen et al. [36]), were both used as indicators to compare the mold proliferation potential and drying capacity of the assemblies.

The experimental tests were performed using the setup that is presented in Figure 2. It consisted of two climate chambers between which a wall sample could be installed, which was designed and built by Mecanik (Montreal, QC, Canada). The chambers had an approximate volume of 17 m^3 each and the wall samples measured 2.6 m by 2.4 m. The temperature, RH and pressure could be controlled independently in each chamber. All samples were anchored to the chambers using lag bolts and were insulated with Rockwool semi-rigid insulation that was 150 mm thick and XPS that was 38 mm thick on the edges to limit the side effects.

The airtightness was tested prior to installing the wall specimens between the chambers to limit the risk of damaging the air barrier layer with the lag bolts that were used to anchor the specimens to the chambers. To test this, a self-adhesive membrane was installed around the wall contours to prevent air exfiltration by any path other than through the assembly.

The details of the tested assemblies are shown in Figure 3. They were designed to perform comparably to an A140OX38 wall, which was the reference assembly as it is currently largely considered to be the most energy efficient option within Quebec's residential construction sector. The walls were named according to their external sheathing, insulation type and thickness. For example, the letter O was used for oriented strand board (OSB), the letter X was for extruded polystyrene (XPS) and the letters F and W were for fiberboard sheathing and Rockwool board insulation, respectively. The first number indicated the thickness of the structural cavity, while the second and third numbers indicated the thickness of the external insulation and the intermediate sheathing panel, respectively. Temperature and RH sensors were positioned within the assemblies, as shown in Figure 3. The sensors are described in Section 2.1.

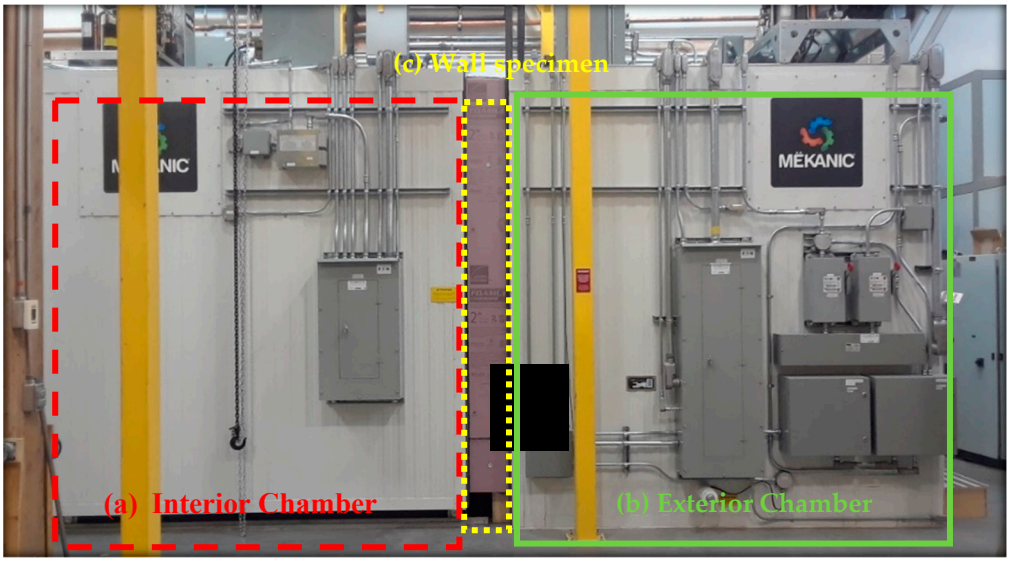

Figure 2. The experimental setup comprising (**a**) a climate chamber reproducing normal indoor conditions, (**b**) a climate chamber reproducing outdoor winter conditions and (**c**) a wall specimen that was covered with insulation to limit the heat transfer to the outside of the laboratory.

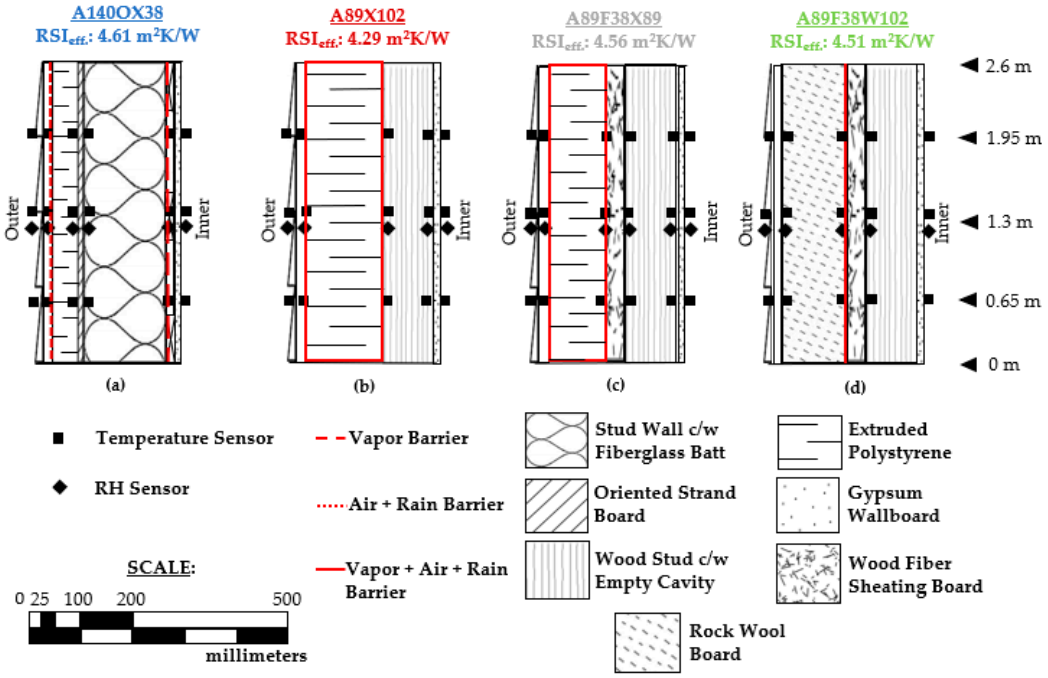

Figure 3. (**a**) An A140OX38 assembly, which is composed of a 140-mm insulated structural cavity with 38-mm extruded polystyrene, an internal vapor barrier and an external rain and air control layer; (**b**) an A89X102 assembly, which is composed of an 89-mm non-insulated structural cavity and 102-mm extruded polystyrene that acts as a thermal, vapor, rain and air control layer; (**c**) an A89F38X89 assembly, which is composed of an 89-mm non-insulated structural cavity, 38-mm fiberboard and 89-mm extruded polystyrene that acts as a thermal, vapor, rain and air control layer; (**d**) an A89F38W102 assembly, which is composed of an 89-mm non-insulated structural cavity, 38-mm fiberboard and 102-mm semi-rigid Rockwool board. The effective thermal resistance was calculated according to the method that was presented by the Government of Canada [37].

The amount of insulation in the assemblies was adjusted so that each assembly had a similar calculated thermal resistance, according to the data from the material manufacturers. Table 1 shows the thermal resistance values of the materials that were provided by the

manufacturers, as well as the calculated effective thermal resistance values of the insulation layers of the assemblies, according to the Government of Canada's calculation method.

Table 1. The thermal resistance values of the materials, as provided by the manufacturers, and the calculated effective thermal resistance values of the insulation layers.

Assembly	Material	Thermal Resistance, According to the Material Manufacturer (m^2K/W)	Calculated Effective Thermal Resistance Value of the Insulation Layer (m^2K/W)
A140OX38	Fiberglass Batt	3.23	4.04 **
	Wood Stud	1.19 *	
	Extruded Polystyrene	1.32	
A89X102	Extruded Polystyrene	3.52	3.52
A89F38X89	Fiberboard	0.71	3.79
	Extruded Polystyrene	3.08	
A89F38X102	Fiberboard	0.71	3.74
	Rockwool Board	3.03	

* This value was taken from the Canadian National Building Code (CNBC) [38]; ** this calculation was performed using the theoretical area percentages of 11% wood and 89% fiberglass insulation in the structural cavity, then the thermal resistance of extruded polystyrene was summed.

2.1. Characterization of the Thermal Conductivity of the Insulation Materials

The samples of the main insulation materials that were used in each assembly were tested using a FOX 314 heat flow meter to determine their thermal conductivity, according to ASTM C518 [39]. The thermal conductivity was determined for three different temperature differentials: 0 to 25 °C, 10 to 35 °C and 20 to 45 °C. The results that are presented in this article were the average of the three thermal conductivity values and the associated relative errors were determined by looking at the largest difference between the average conductivity value and the three individual conductivity values from the tests.

The effective thermal resistance of the insulation layers was calculated by using the thickness and thermal conductivity of each material to determine its thermal resistance and then summing the thermal resistance of each material within the assembly. To measure the impact of the external insulation approach, the following equation was used for the discontinuous layers in the A140OX38 assembly, in which the insulation was between the studs:

$$RSI_{parallel} = 100/\left((\%A_f/RSI_f) + (\%A_c/RSI_c)\right) \quad (1)$$

where $\%A_f$ is the framing surface percentage, $\%A_c$ is the cavity surface percentage, RSI_f is the thermal resistance of the framing layer and RSI_c is the thermal resistance of the cavity layer. All thermal resistances were in m^2K/W.

2.2. Characterization of the Temperature and RH Profiles of the Wall Assemblies under Cold Weather Conditions

To determine the temperature and RH profiles of the assemblies, specimens were placed between the chambers for 7 days and fixed temperature conditions were maintained in both chambers to reach a steady state. The results that are presented were the averages of the hourly data that were obtained during the first 24 h after the 7 days of the experiment. The interior chamber was calibrated to a temperature of 21 °C and an RH of 40%, while the exterior chamber was calibrated to a temperature of −18 °C and an RH of 50%. The temperature and RH profiles that were measured were compared to those that were obtained using WUFI under the same temperature and RH conditions. For comparison purposes, the effects of wind pressure, rain and radiation on the temperature and RH profiles were not considered in the WUFI simulations.

Omega RTD temperature sensors (model NB-PTCO-006) were installed on the internal side of the sheathing material in the assemblies. The probes were calibrated using a Fluke

1524 dual-channel reference thermometer. A sensor precision of ± 0.3 °C was obtained for temperatures from −20 °C to 60 °C. The calibration was performed using multipoint slope correction in comparison to the Fluke 1524 temperatures at −10 °C, 0 °C, 10 °C, 20 °C, 30 °C, 40 °C, 50 °C and 60 °C and slope correction by calculation at −30 °C and 80 °C.

Honeywell humidity sensors (model HIH-4000-001) were also installed between the insulation layers in the assemblies. In addition to characterizing the moisture transfer within the assembly, these sensors made it possible to analyze the risk of condensation in conjunction with the temperature measurements. They were calibrated using Vaisala HMI41 and HMP42 sensors. The sensor precision was ± 2% for RH values from 20% to 80%. The calibration was performed using multipoint slope correction in comparison to the Vaisala HMP42 sensor results at 20%, 40%, 50%, 60% and 80% RH and slope correction by calculation at 15% and 95% RH.

2.3. Characterization of the Airtightness of the Assemblies

A sealed box, as shown in Figure 4, was built and attached to the inner side of each wall assembly. The box was equipped with an air supply cable and an MPR 500 pressure meter from Kimo Canada, which could measure pressure differentials between 0 and 500 Pa. The air supply cable was also connected to an F-112AC-M20 flow meter from Bronkhorst to measure the airflow rate at any moment during the experiment. The flow meter could measure airflow rates from 0.167 L/s to 4.17 L/s with an accuracy of ±0.5% on the reading scale and ±0.1% on the full scale.

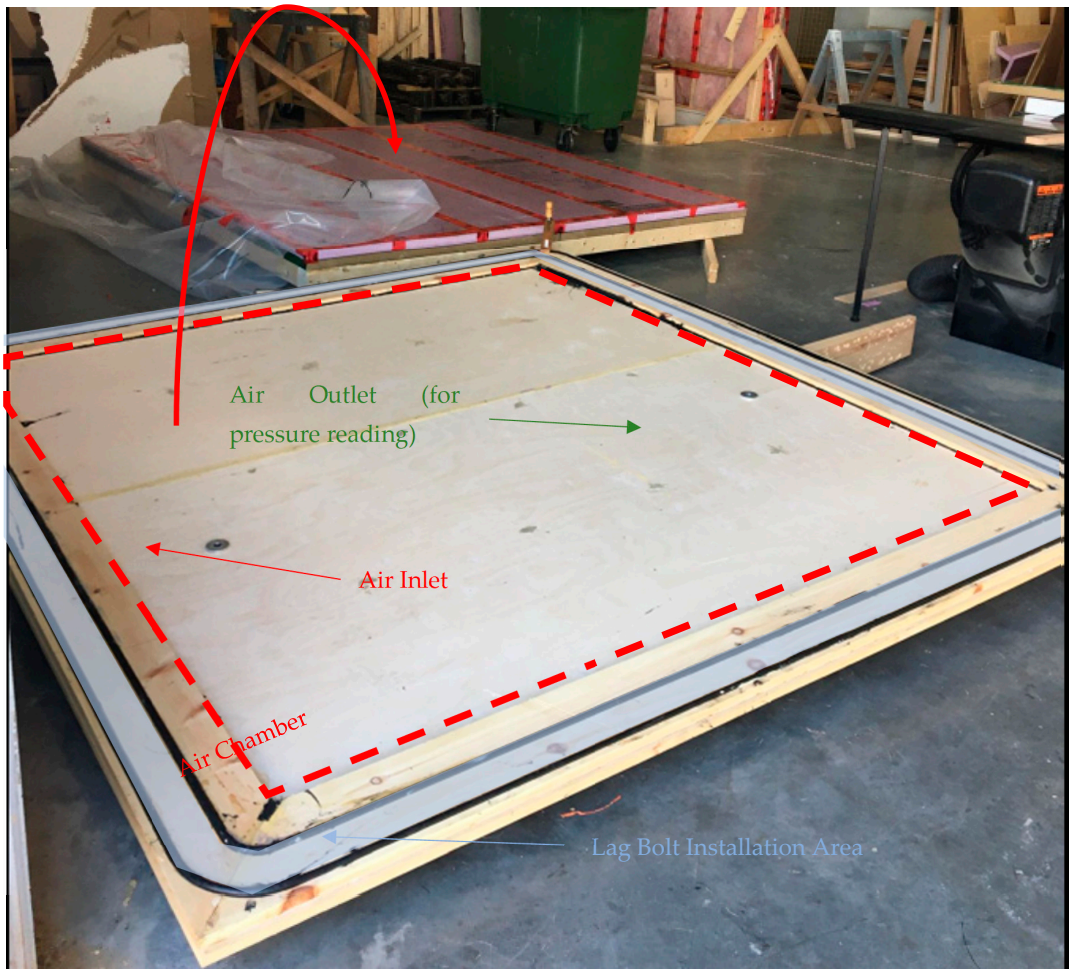

Figure 4. The sealed box that was used for the airtightness testing. The box was attached to the wall assembly using lag bolts and rubber washers. An air outlet and air inlet were installed to allow air to enter the air chamber and to measure the pressure in the chamber.

The box covered 5.3 m^2 of the wall surface. The procedure that was used to measure air permeability was as follows. First, two sheets of polyethylene were taped to the inside of the wall assembly and then, the sealed box was fixed to the assembly using lag bolts to seal the joint between the box and the polyethylene as tightly as possible. Extraneous air leakage, i.e., the air leaving the chamber that did not pass through the tested specimen, was measured at the following pressure differentials: 25, 50, 75, 100, 150 and 300 Pa. The polyethylene was then removed and the six measurements were repeated. After a value of 300 Pa was reached, air leakage was remeasured at 100, 75 and 50 Pa to determine whether the measurement process had affected the air leakage. Only overpressure was measured, as the external cladding did not allow for the efficient sealing of the box.

The uncertainty that was due to variations in air density as a function of the temperature was considered in accordance with the guidelines of the flow meter manufacturer. The uncertainty in the measurement of the extraneous air leakage was a function of the accuracy of the flow meter and the consistency of the leakage from one test to the next. The uncertainty of the total leakage rate measurement was a function of the air leakage between the self-adhesive membrane and the contour of the wall assembly that was being tested and the consistency of the measurements that were taken at the same pressure. The uncertainties in the results were calculated according to Annex A1 of the ASTM E783-02 standard [40].

2.4. Measurement of the Airborne Sound Transmission Loss

The airborne sound attenuation through the assembly was measured according to the ASTM E336-19A standard [41]. Although the method that is described in the standard was followed, the volume of the chambers did not meet the standard's minimum volume requirements (an actual volume of 17 m^3 versus the recommended 25 m^3 in the standard). The reverberation time in the receiving room, which was required to calculate the noise reduction between the two chambers, was chosen to remain constant at 0.5 s because the volume of the chambers was small. This practice was considered to be acceptable for the assembly comparison purposes. For these reasons, the results that are stated in this study only represent the specific construction and acoustic conditions at the time of the test. The ASTM E413 standard was then used to calculate the apparent sound transmission class (ASTC) [42]. An uncertainty of 1 ASTC was considered for all measurements to take into consideration the non-compliance of the chamber volume.

2.5. Hygrothermal Simulations

WUFI Pro is used to perform one-dimensional hygrothermal transfer simulations considering various factors, such as initial material moisture content, solar radiation, rain, wind and condensation. WUFI Pro version 6.5 developed by the Department of Hygrothermics at Fraunhofer IBP (Stuttgart, Germany) was used in this work. The software can also model ventilated air cavities, air leakage and rain penetration using the source and sink function. The hygrothermal simulations provided data to compare the sheathing water contents and mold growth index values from different scenarios.

We used the simulations to evaluate whether the wall assemblies had acceptable mold proliferation index and sheathing water content values when subjected to:

1. Normal exposure, which corresponded to 1% rain infiltration on the backside of the external cladding and a sheathing flanking flow of 0.02 $L/s \cdot m^2$ through the assembly using the source and sink approach, with an initial sheathing moisture content of 80%;
2. Unfavorable exposure, which corresponded to 1% rain infiltration on the backside of the external cladding and 0.01% infiltrating into the sheathing and airflow of 0.02 $L/s \cdot m^2$ through the assembly using the source and sink approach, with an initial sheathing moisture content of 80%;
3. Very unfavorable exposure, which corresponded to 1% rain infiltration on the backside of the external cladding and 0.1% infiltrating into the sheathing and an airflow of 0.02 $L/s \cdot m^2$ through the assembly using the source and sink approach and an initial

sheathing moisture content of 250 kg/m^3 to verify the resilience of the assemblies when subjected to severe humidity conditions.

The mathematical mold growth model that was developed by Hukka and Viitanen [35] and was more recently improved by Ojanen et al. [36] was used in this study to evaluate the risk of mold growth. The model, which is available via the WUFI Mold Index VTT add-ons, was developed according to the researchers' work and led to the recent addition of Addendum E to the ASHRAE 160 standard [43]. Glass et al. [44] conducted a comparative study of the 30-day criterion method (which was used in the older versions of the ASHRAE 160 standard to measure the moisture performance of assemblies) and Viitanen's mold growth model. Their study showed that the mold growth model provided more reliable predictions compared to field observations. The 30-day criterion method requires that the 30-day running average for RH at the material surface be below 80% when the 30-day running average for surface temperature is between 5 °C and 40 °C [44]. The mold growth model, on the other hand, provides an assessment of the risk of mold growth within a component of an assembly by considering the material's sensitivity to mold, its RH and its temperature. The mold growth index was thoroughly explained by Hukka and Viitanen [35].

The source and sink approach was used in the model to represent the airflow through the assembly, as described by Lstiburek [45]. Two 5-mm airspaces were created on the backside of the sheathing: one coupled to external air using the air exchange function and the other coupled to internal air. An airspace that was coupled to external air was also added on the inner side of the sheathing to act as cladding ventilation. A value of 0.05 L/s·m^2 was set for the gap on the inner side of the sheathing. To accommodate the WUFI source and sink function, various flows were added into the air change per hour values and converted, according to Lstiburek's work [45] and the ASHRAE 1091 research project [46].

The simulations were conducted for two different locations in Quebec, Canada, (see Table 2) that have different climates: Kuujjuaq, which has a subarctic climate, and Montreal, which is in the south of the province and has a cold climate. Table 2 presents the number of heating degree days at each site (with a base temperature of 18 °C), according to the NBC.

Table 2. The number of heating degree days (base temperature: 18 °C) at the two different locations that were considered in this work, which ranges from cold to subarctic climates.

Location	Number of Heating Degree Days
Montreal	4470
Kuujjuaq	8550

Climate data were extracted from Canadian Weather Files for Energy Calculation (CWFEC), which is a dataset that was created by concatenating 12 typical weather months that were selected from a database of Canadian Weather Energy and Engineering Datasets (CWEEDS), covering up to 30 years.

The daily precipitation data for the 12 typical weather months were added to this dataset from the WAC file export dataset that was provided by WUFI. The internal temperature and RH values were extracted from data that were recorded in the case study of a building in Quebec City, which was used to study the impact of occupant behavior on building energy efficiency [47]. We used the averages of the temperature and RH values that were obtained over one year from various apartments that were equipped with sensors.

The material properties of the wall components that were used in the WUFI simulations are presented in Table 3. For the Kuujjuaq climate, the thickness of the insulation was modified to meet the QCC criteria [5]: 12.7 mm of XPS was added to the 140OX38 assembly, 25.4 mm of XPS was added to the E89X102 and E89F38X89 assemblies and 25.4 mm of Rockwool board was added to the E89F38W102 assembly.

Table 3. The properties of the materials that were used for the simulations.

Material	Density (kg/m^3)	Porosity (m^3/m^3)	Heat Capacity (J/kg·K)	Thermal Conductivity (W/m·K)	Diffusion Resistance Factor (-)
Gypsum	625	0.706	870	0.16	7.03
Polyethylene	130	0.001	2300	2.3	32,800
Fiberglass	11.5	0.999	840	0.043	1.21
OSB	650	0.95	1880	0.092	812.5
XPS	28.6	0.95	1470	0.03	100
Polyethylene Fiber Air Barrier	130	0.001	2300	2.3	297
Cedar Cladding	350	0.8	1880	0.084	1963
Spruce	400	0.9	1880	0.086	552
Fiber Board	265	0.8	1400	0.054	2.94
Rockwool Board	128	0.954	850	0.0322	1.3

3. Results

3.1. Thermal Resistance of the Insulation Materials, as Calculated from Their Thermal Conductivity

Table 4 presents the thermal conductivity results for each of the insulation materials that were used in the wall assemblies, as well as the calculated thermal resistance and the effective thermal resistance of the insulation layers in each assembly.

Table 4. The effective thermal resistance of the whole wall, the thermal resistance of the insulation materials and the thermal conductivity, as measured in the laboratory using a FOX 314 heat flow meter.

Assembly	Material	Material Thickness (mm)	Thermal Conductivity (W/m·K)	Material Thermal Resistance (m^2K/W)	Insulation Layers Effective Thermal Resistance (m^2K/W)
A140OX38	Fiberglass Batt	140 ± 1	0.041 ± 0.003	3.4 ± 0.3	4.1 ± 0.5 *
	Wood Stud	140 ± 1	0.099 ± 0.008	1.4 ± 0.3	
	Extruded Polystyrene	38.1 ± 0.5	0.031 ± 0.003	1.2 ± 0.2	
A89X102	Extruded Polystyrene	102 ± 1	0.031 ± 0.003	3.3 ± 0.4	3.3 ± 0.4
A89F38X89	Fiberboard	38.1 ± 0.5	0.089 ± 0.007	0.4 ± 0.1	3.3 ± 0.4
	Extruded Polystyrene	88.9 ± 0.5	0.031 ± 0.003	2.9 ± 0.3	
A89F38X102	Fiberboard	38.1 ± 0.5	0.089 ± 0.007	0.4 ± 0.1	3.5 ± 0.4
	Rockwool Board	102 ± 1	0.033 ± 0.003	3.1 ± 0.3	

* This calculation was performed using the theoretical area percentages of 11% wood and 89% fiberglass insulation for the structural cavity, then the thermal resistance of extruded polystyrene was summed.

The thermal resistance was calculated by dividing the thermal conductivity of each material by its thickness. When materials were layered against each other, their overall thermal resistance was determined by summing their individual values. As mentioned in Equation (1), when two materials were alternated within the same layer, the effective thermal resistance was calculated using the isothermal method. The effective thermal resistance of the structural cavity of the A140OX38 assembly was calculated based on the area percentage of each material, as stipulated in the CNBC [38]. The thermal resistance value that is shown in Table 2 for the A140OX38 assembly considered wood studs that were spaced 610 mm apart, which equated to the area percentages of 11% wood and 89% fiberglass insulation, according to the CNBC [38].

Table 4 also shows the effective thermal performance of the insulation layers that were used in each assembly. The A140OX38 assembly was found to have the highest thermal resistance at 4.1 ± 0.4 m^2K/W, while the A89F38X89 and A89X102 assemblies both had a thermal resistance of 3.3 ± 0.4 m^2K/W and the A89F38X102 assembly had a thermal resistance of 3.5 ± 0.4 m^2K/W. The calculation for the effective thermal resistance of the

A140OX38 assembly was 11% lower than the total thermal resistance that was calculated in the center of the thermal insulation due to the thermal bridging that was generated by the repetition of the studs. The measured thermal resistance of the fiberboard and XPS was lower than that proposed by the manufacturers of these materials, which affected the thermal resistance of the insulation layers, especially in the E89X102 and E89F38X89 assemblies. On the other hand, the thermal resistance of the Rockwool board and fiberglass was higher than the values that were presented by the manufacturers of these materials, which positively affected the thermal resistance of the insulation layers of the E140OX38 and E89F38W102 assemblies.

3.2. Temperature and RH Profiles under Cold Weather Conditions, as Obtained from Laboratory Experiments and WUFI Simulations

Sheathing temperature is often used to predict the performance and durability of a wall. The article "The Hygrothermal Performance of Exterior Insulated Wall Systems" suggested that exposing sheathing to high temperatures leads to accelerated organic material breakdown. Exposure to large temperature variations over multiple short periods of time can cause movement, stress and fatigue, which all affect the durability of the materials that form these layers [25]. Although the RH conditions were specified, the results showed that the RH in the chambers varied considerably and oscillated around the values that were set. The RH varied between 30% and 50% in the interior chamber and between 45% and 70% in the exterior chamber, with these oscillations being due to the operation of the humidifiers and radiators inside the chambers. Figure 5a–d show the temperature and RH profiles that were obtained for each wall assembly from the climate chambers after 7 days and the comparative profiles that were obtained from the WUFI simulations. The calculation of the dew point of the indoor air was also added to the figures to indicate where potential interior air exfiltration could lead to condensation within the composition of each assembly.

As expected, the experimental and WUFI simulation measurements suggested that the interior temperature of the OSB in the A140OX38 assembly stabilized at slightly below 0 °C. The RH value that was obtained from the laboratory measurements was 70%, which was higher than the RH of the internal sheathing in the other assemblies (which was between 55% and 40%). These observations were consistent with Craven and Garber-Slaght's work on the influences of the amount of insulation outside of a framing cavity and the corresponding RH inside the sheathing [26], as well as most other studies about the effects of external insulation on the RH of internal sheathing in cold climates [24,37,38]. The position of the dew point inside the cavity explained the increase in RH for this assembly and showed that condensation on the backside of the OSB was likely to occur.

The WUFI simulation results proposed temperature profiles that were similar to those that were obtained from the laboratory testing. The differences between the RH profiles, especially those of the A140OX38 and A89F38W102 assemblies, were on the outside of the assemblies and were due to fluctuations in the RH of the exterior climate chamber. On the external surface of the fiberboard of the A89F38W102 assembly, an RH value of 64% was obtained from the WUFI simulation, whereas the value that was obtained in the laboratory differed by 15%. The difference between the vapor diffusion resistance of the fiberboard used in WUFI and that used in the laboratory could affect these results. Further research is needed to confirm this hypothesis.

The A89X102 assembly had a higher RH in the laboratory tests than the A89F38X89 and A89F38W102 assemblies, which was directly related to the higher RH in the interior climate chamber. These results suggested that when a vapor barrier was used on the exterior of the structural cavity that was made of wood studs and no polyethylene was used as an interior vapor barrier, the RH on the interior of the sheathing was very similar to the RH in the interior chamber. These results were consistent with those of Trainor, T. [25]. As suggested in the article on the "perfect wall", using a semi-permeable finish on the internal surface of the assembly reduced the dependency of the inner surface of the sheathing on the interior chamber RH, without inhibiting the assembly's ability to dry from the interior through the

control layers [21,29]. Furthermore, the less insulation that was installed on the outside of the cavity in the A140OX38 assembly, the more sensitive the OSB's temperature was to the outside temperature. The dew point position for the externally insulated assemblies was within the insulation layer for all assemblies, indicating that under these conditions, no condensation formed on the interior of the cavity, even when there was air exfiltration from the interior to the assembly components. The position of the dew point could be modified by an increase in the inside RH, which could cause the dew point to move inside the structural cavity. Nevertheless, interior RH levels under winter conditions are generally very low [48], although RH levels of 50% and more may occur [49].

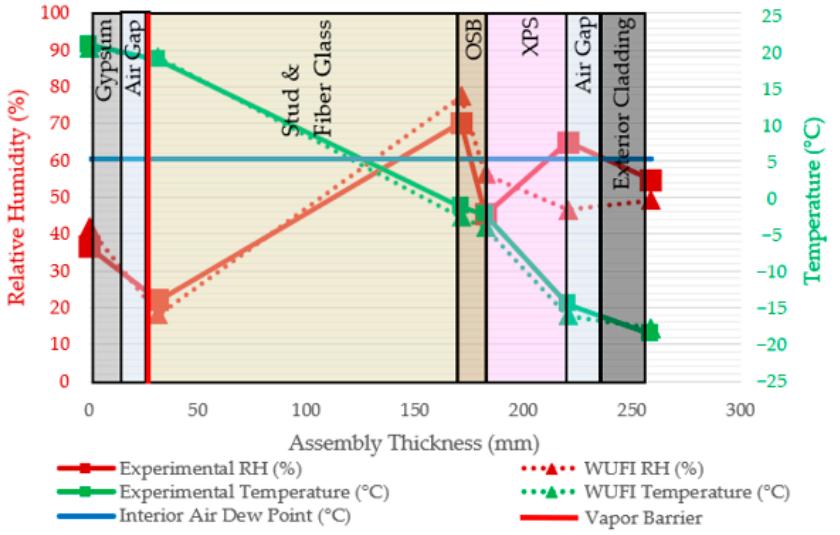

(**a**)

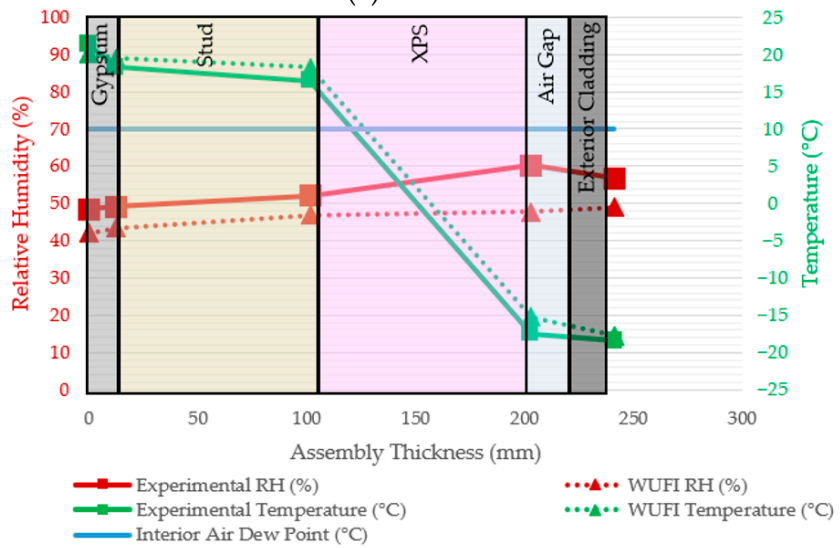

(**b**)

Figure 5. *Cont.*

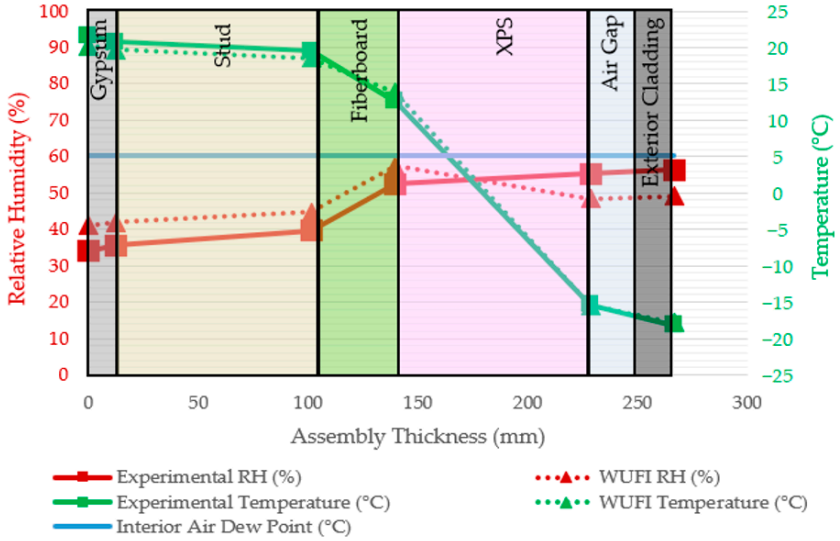

(**c**)

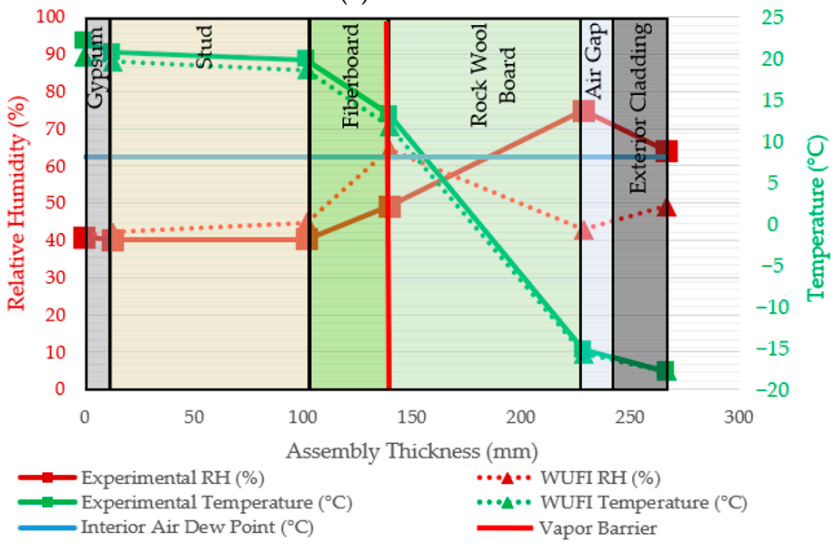

(**d**)

Figure 5. The temperature, calculated experimental interior air dew point and RH profiles for the tested assemblies: (**a**) A140OX38; (**b**) A89X102; (**c**) A89F38X89; (**d**) A89F38W102.

3.3. Measurement of Airflow through the Assemblies

Figure 6 presents the airtightness results for the various assemblies. It shows that considerably less air leaked through the assembly that used XPS as its main air barrier. The rate of air leakage at 75 Pa was used as the basis for comparison. The air leakage per unit of surface area was 0.17 L/s·m^2 ± 10% at 75 Pa for the A89F38X89 and A140OX38 assemblies and 0.33 L/s·m^2 ± 6% at 75 Pa for the A89F38W102 assembly. To try to optimize the E89F38W102 assembly, a final test was conducted by modifying theA89F38W102 assembly to incorporate a 1.35-mm modified bitumen SBS membrane rather than a polyethylene membrane. The objective of this change was to observe whether this type of membrane could seal the connectors and make it possible to fasten furring strips to wood studs. This modified assembly had an air leakage rate of 0.27 L/s·m^2 ± 7% at 75 Pa, suggesting a superior airtightness than the A89F38W102 assembly (which had a polyethylene membrane). However, the modified assembly was not as airtight as the assemblies with air-sealed rigid panels. The air leakage was not measured at 300 Pa for either assembly, since the maximum flow meter measurement value was reached before that pressure value. The sources of the errors were related to the flow meter and pressure sensor readings.

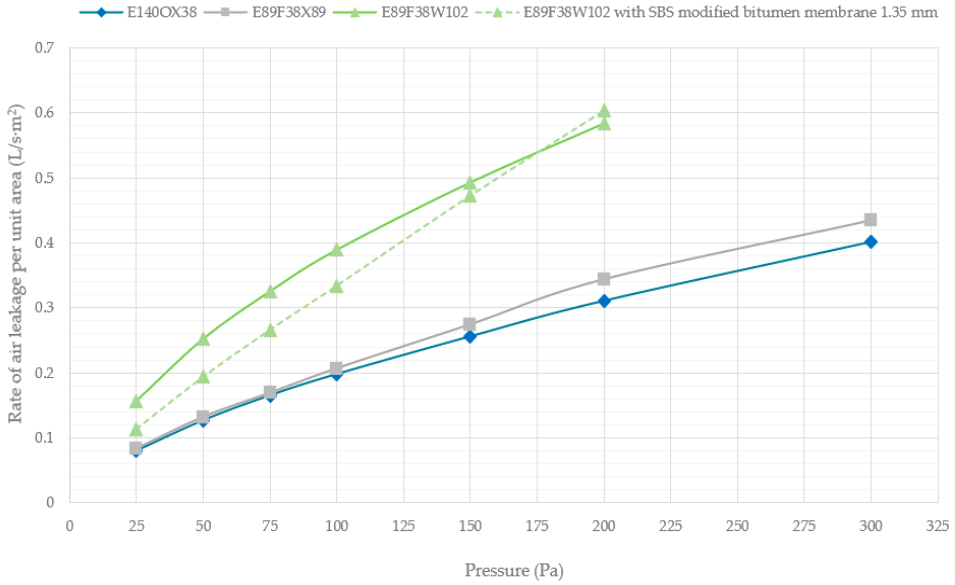

Figure 6. The air leakage that was measured through the A140OX38, A89F38X89 and A89F38W102 assemblies and the A89F38W102 assembly, which was fitted with a modified bitumen SBS membrane.

The results showed similar trends to those found by Hun et al. [50], who proved that assemblies with air barriers that are composed of XPS offer superior airtightness than assemblies with air barriers that are composed of polyethylene or high-density polyethylene fiber membranes. However, the results themselves differed between our study and the other. The A140OX38 assembly had a 2.4 times higher air infiltration rate per unit area in this study than in Hun et al.'s study. Similarly, theA89X102 assembly, which featured XPS panels as the air barrier, had an 8.5 times higher air infiltration rate in this study than in Hun et al.'s study. On the other hand, theA89F38W102 assembly, which had an interior polyethylene air barrier, had a 2.1 times lower air infiltration rate in this study than the similar assembly in Hun et al.'s study. According to our analysis of Hun et al.'s study, the notable discrepancies between the results of the two studies were mainly due to the quality of the details of the assembly designs and the fact that the researchers in Hun et al.'s study could make modifications based on preliminary tests. For example, using screws and caps with 2-inch diameters for the assembly with an external polyolefin membrane helped to limit the air infiltration through the connectors. Using a cap with a 1-inch diameter, as in this study, resulted in an air infiltration path being created when the cap flexed under pressure. In addition, the presence of several infiltration paths in Hun et al.'s study that were not measured in this study, such as electrical boxes and PVC pipes, increased the difficulty of sealing the air barriers and explained the higher air infiltration rates that were obtained in Hun et al.' study.

3.4. Airborne Sound Transmission Class

As shown in Table 5, the ASTC value of the A140OX38 assembly was 49 ± 1. The ASTC was significantly influenced by the removal of the insulation in the stud cavity and by the replacement of fiberglass wool with solid XPS, as the ASTC value of the A89X102 assembly was 40 ± 1. The noteworthy difference between the transmission loss values of the two assemblies was mainly due to the loss of mass from removing the OSB panel and the use of 89 mm × 38 mm studs, which were lighter than 140 mm × 38 mm studs. Removing the insulation from the cavity also reduced the transmission loss of the A89X102 assembly since fiberglass wool, which acts as an absorptive infill, was not used. The addition of fiberboard was the first material choice that was made to optimize the sound transmission loss. The fiberboard contributed to an increase in the ASTC value of the A89F38X89 assembly to 45 ± 1. The fiberboard that was used in theA89F38X89 assembly acted as an absorbent panel and increased the mass of the assembly. In the A89F38W102 assembly, a second

choice to optimize the A89F39X89 assembly was made by adding a Rockwool semi-rigid board instead of the rigid XPS board. The increased transmission loss that was provided by the fiberboard was maintained. In addition, the semi-rigid Rockwool panels that were used acted as a porous absorber and enabled the assembly to achieve an ASTC value of 50 ± 1, which was comparable to that of the A140OX38 assembly.

Table 5. The ASTC ratings of the tested assemblies.

Assembly [1]	Material	Material Thickness (mm)	ASTC Ratings
A140OX38	Fiberglass Batt	140 ± 1	49 ± 1
	Extruded Polystyrene	38.1 ± 0.5	
A89X102	Extruded Polystyrene	102 ± 1	40 ± 1
A89F38X89	Fiberboard	38.1 ± 0.5	45 ± 1
	Extruded Polystyrene	88.9 ± 0.5	
A89F38X102	Fiberboard	38.1 ± 0.5	50 ± 1
	Rockwool Board	102 ± 1	

[1] All assemblies had a 12.7-mm interior gypsum layer and studs that were spaced at 400 mm c/c.

3.5. Hygrothermal Simulations

Sheathing water content data were extracted from the simulations and mold growth indices were calculated using the WUFI Mold Index VTT add-ons.

3.5.1. Performance, According to Sheathing Water Content

Table 6 shows the sheathing water contents (or the stud water content for the A89X102 assembly) when the assemblies had an orientation that faced west since the wind directed rain toward the wall in greater quantities in that direction. The table shows the results for Kuujjuaq's subarctic climate and Montreal's cold climate. The cells in the table are color coded to make the table easier to read. Water contents that were less than 15% are in green, water contents that were between 15% and 19% are in yellow and water contents that were greater than 19% are in red.

Table 6. The highest water contents during the second year of simulation as a function of the conditions and climate of the wall exposure.

Exposure/Climate	Highest Water Content (%) During the Second Year of Simulation *			
	Assembly (Material)			
	A140OX38 (OSB)	A89X102 (Wood Stud)	A89F38X89 (Fiberboard)	A89F38W102 (Fiberboard)
Normal Exposure/Subarctic Climate	12%	6%	9%	9%
Unfavorable Exposure/Subarctic Climate	12%	6%	9%	9%
Highly Unfavorable Exposure/Subarctic Climate	21%	18%	9%	9%
Normal Exposure/Cold Climate	9%	6%	8%	8%
Unfavorable Exposure/Cold Climate	10%	6%	8%	8%
Highly Unfavorable Exposure/Cold Climate	33%	20%	9%	9%

* The highlighting in green of boxes indicates a water content under 15%, the highlighting in yellow indicates a water content between 15% to 19% and the highlighting in red indicates a water content over 19%.

The results suggested that the moisture contents of the sheathing and wood studs remained low under normal or unfavorable exposure conditions for all assemblies. The moisture content did not exceed 9% for the A89F38X89 and A89F38W102 assemblies under any exposure conditions. The RH of these assemblies was primarily governed by the RH inside the building since the vapor barrier was on the outside of the sheathing or timber

stud. When the RH inside the building varied between 30% and 60%, the sheathing was subject to a low humidity content that made it possible for the assembly to dry within a year when subjected to a high water content at the beginning of the simulation. Variations in the exterior RH and temperature had little impact on the drying of the sheathing due to the thermal insulation and vapor barriers being installed on the outside. Therefore, the climate zone in which the wall was located had minimal impact on the condition of this layer. The water infiltration that was applied to this layer also had little impact on the water content of the fiberboard since the water content remained at 9%. The difference between the fractions of rainwater that were applied to this layer under unfavorable and highly unfavorable exposure conditions did not significantly impact the water content of the panel. The same observations were made when the A140OX38 and A89X102 assemblies were subjected to unfavorable exposure conditions. The results for the A89X102 assembly suggested that the maximum moisture content of the wood studs was 18% in the subarctic climate and 20% in the cold climate when subjected to highly unfavorable exposure conditions. The moisture content of the wood studs in the second year of the simulation was impacted by drying time when they were subjected to an initial moisture content of 250 kg/m^3. The difference between the moisture content when subjected to the cold climate versus when subjected to the subarctic climate was associated with the amount of water that fell on the wall, which was greater in the cold climate. The A140OX38 assembly had the highest sheathing water content when subjected to highly unfavorable exposure conditions. The moisture content of the OSB panel was 21% in the subarctic climate and 33% in the cold climate during the second year of the simulation.

Figure 7 shows the evolution of the water content of the sheathing in the A140OX38, A89F38X89 and A89F38W102 assemblies and the wood studs in the A89X102 assembly for the full duration of the simulation under highly unfavorable exposure conditions in the cold climate.

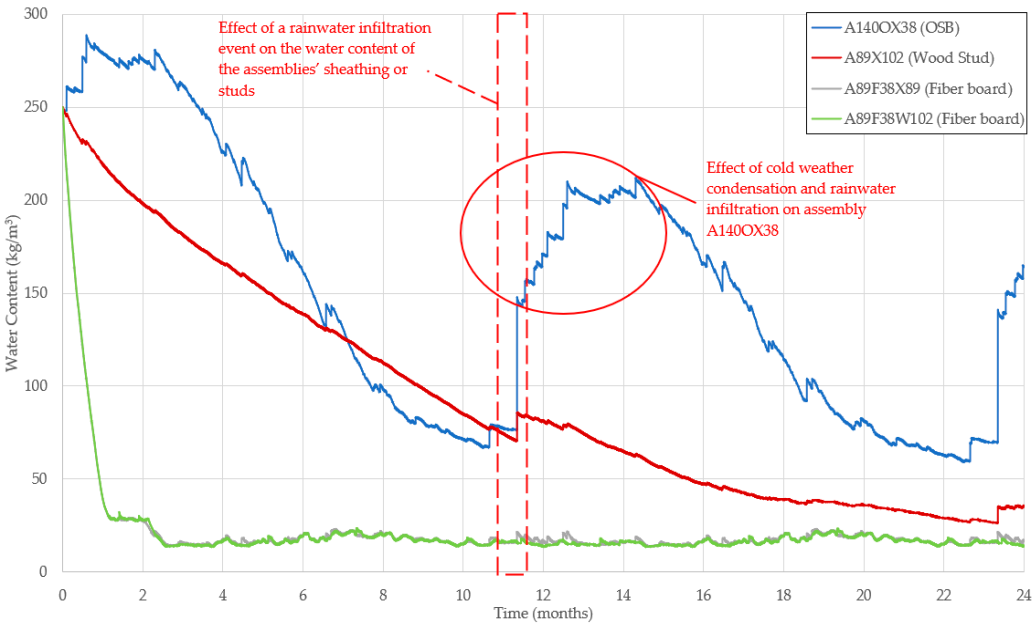

Figure 7. The sheathing or wood stud water contents for the full duration of the simulation under highly unfavorable exposure conditions in the cold climate.

It was possible to compare the drying rates of the sheathing or wood studs of the assemblies during the first 12 months of the simulation when their initial moisture content was 250 kg/m^3. The results indicated that the A89F38W102 and A89F38X89 assemblies had a high drying rate as only 664 h was required for their fiberboard panels to reach a moisture content of 51.6 kg/m^3 (19%). In comparison, the A89X102 and A140OX38 assemblies required 7705 h and 5160 h, respectively, to reach the same moisture level. The results for

the A89X102 assembly did not consider the drying capacity of the cavity between the wood studs since the simulation was performed in one dimension. Therefore, the simulation underestimated this assembly's drying capacity.

The area in Figure 7 that is framed by the red dashed line shows the effects of a water infiltration event on the water contents of the sheathing or wood studs (in the case of the A89X102 assembly) of the assemblies. The simulations suggested that when the assemblies were subjected to heavy rainwater infiltration, the impact of the infiltration was more significant for the A140OX38 assembly since the moisture content of the OSB panel increased from 70.5 kg/m^3 (12%) to 147.9 kg/m^3 (23%). The impact was less pronounced for the A89X102 assembly, whose stud moisture content increased from 70.5 kg/m^3 (18%) to only 86.0 kg/m^3 (21%), whereas the sheathing water content of the A89F38X89 assembly increased from 15.9 kg/m^3 (6%) to 21.7 kg/m^3 (8%) and the sheathing water content of the A89F38W102 assembly remained unchanged at 16.1 kg/m^3 (6%). The hygroscopic nature of OSB was responsible for the significantly different response of the A140OX38 assembly compared to the other assemblies. The combination of the high RH in winter and the rain event caused a substantial increase in the water content of the fiberboard since the material's hygroscopicity was marked by a steep increase in water content when subjected to an RH approaching 100%. The area in the red circle in Figure 7 shows the impact of winter condensation on the water content of the OSB sheathing of the A140OX38 assembly. The results indicated that the panel's water content increased from 147.9 kg/m^3 (23%) to 210.2 kg/m^3 (32%) in the presence of winter condensation, whereas the moisture contents of the fiberboards and studs of the other assemblies remained unimpacted by winter condensation as no condensation was observed. These fluctuations were due to having less thermal insulation outside the structural cavity and the temperature of the OSB panel being below the air dew point inside the structural cavity during winter.

As in Smegal and Straube's work [24], using a polyethylene sheet on the interior as a vapor barrier limited the occurrence of high sheathing moisture levels and using more external insulation tended to decrease the sheathing moisture content. When the study model from Smegal and Straube included a percentage of rainwater infiltration, the moisture content of the sheathing was a function of the amount of infiltrated water, the outside temperature and the drying capacity of the assembly. Both Smegal and Straube's study [24] and this work showed that using low-permeance external insulation and a polyethylene interior vapor barrier (as in the A140OX38 assembly) could limit an assembly's drying capacity and increase the risk of mold growth.

3.5.2. Mold Proliferation Risk, Based on the WUFI Mold Index Model

Simulations were used to study the risk of mold growth in the four assemblies that were investigated in two climate zones and under three different exposure conditions, which were presented in Section 2.4. Table 7 shows the mold growth index values for the different exposure conditions and climate zones for a northern orientation.

An analysis of the mold growth index made it possible to include the material in the calculation of that material's sensitivity to mold. The sensitivity class of the intermediate cladding materials and wood studs was selected in accordance with the WUFI mold index VTT classification add-on. The fiberboard in the A89F38X89 and A89F38W102 assemblies was in the highly sensitive class, which includes untreated wood that has lots of nutrients for biological growth. The OSB and SPF wood studs were in the sensitive class.

The results that are presented in Table 7 showed that the mold growth index remained at zero under the normal and unfavorable exposure conditions in both the cold and subarctic climates. The maximum mold growth index values that were obtained during the second year of simulation under highly unfavorable exposure conditions in the subarctic climate were 2.6 and 2.7 for the fiberboard in the A89F38X89 and A89F38W102 assemblies, respectively. An index of 2 to 3 indicates the risk of having minimal visible mold on the surface of the material in question. An analysis of the maximum water content data in Table 6 and the mold growth index values suggested that there was a risk of mold growth

despite having a low water content of 9%. The mold growth index was influenced by the high water content at the beginning of the simulation and by the fiberboard's high sensitivity to mold. Despite the fact that the assemblies dried quickly, the risk of mold growth remained in the second year of simulation. In the cold climate (and under highly unfavorable exposure conditions, as mentioned above), the index values were 3.1 for the A89F38X89 assembly and 3.2 for the A89F38W102 assembly. This increase in the index value was due to the more frequent and abundant precipitation in the cold climate versus that in the subarctic climate. An index of 3 to 4 indicates the risk of mold growth on up to 10% of the panel's surface. The OSB panel in the A140OX38 assembly and the wood studs in the A89X102 assembly had mold growth ratings of 3 and 3.3, respectively, under highly unfavorable exposure conditions in the subarctic climate. The higher index values of these assemblies were explained by their higher water contents during the second year of simulation, which limited the drying capacity of their sheathing material or studs compared to that of the A89F38X89 and A89F38W102 assemblies. Those results remained quite similar, as the OSB panel and the wood studs were more resistant to mold growth. The mold growth index of the OSB panel in the cold climate was 4.4, which was consistent with the detectable growth on 10% to 50% of the panel. This increase could be explained by the high water content in the second year of simulation, which did not allow the panel to dry out and favored conditions that were conducive to mold proliferation. The same observation was made for the A89X102 assembly, for which the index value was 3.7 under highly unfavorable exposure conditions in the cold climate.

Table 7. The highest mold proliferation index during the second year of simulation as a function of the conditions and climate of the wall exposure.

Exposure/Climate	Highest Mold Proliferation Index During the Second Year of Simulation *			
	Assembly (Material)			
	A140OX38 (OSB)	A89X102 (Wood Stud)	A89F38X89 (Fiber Board)	A89F38W102 (Fiber Board)
Normal Exposure/Subarctic Climate	0.0	0.0	0.0	0.0
Unfavorable Exposure/Subarctic Climate	0.0	0.0	0.0	0.0
Highly Unfavorable Exposure/Subarctic Climate	3.0	3.3	2.6	2.7
Normal Exposure/Cold Climate	0.0	0.0	0.0	0.0
Unfavorable Exposure/Cold Climate	0.0	0.0	0.0	0.0
Highly Unfavorable Exposure/Cold Climate	4.4	3.7	3.1	3.2

* The highlighting in green of boxes indicates an index of mold growth between 0 and 2, i.e. no mold growth to very little microscopic growth, the highlighting in yellow indicates an index between 2 and 3, i.e. several localized mold growths on the surface (microscopic) and the highlighting in red indicates an index of more than 3, i.e. a visible growth of mold on a surface from localized to widespread

4. Discussion

The external insulation approach proposes the displacement of the dew point position to the exterior of the structural cavity. The externally insulated assemblies that were studied in this project had vapor profiles (see Figure 5b–d) that supported this idea because the RH values remained low in the structural layers inside the cavities during the climate chamber testing and increased in the thermal insulation layers outside the cavities. The simulations showed a similar trend when the assemblies were subjected to the same temperature and RH conditions. The effects of temperature variations and external humidity on the structural components of the assembles were limited due to the absence of thermal insulation inside the cavities and the presence of vapor barriers and air barriers on the outside of the cavities. The structural components were primarily influenced by the climactic conditions inside the building. The effectiveness of externally insulated assemblies was dependent on the ability of the building occupants to maintain a normal RH of under 60% to limit the risk of the degradation of the assembly components. In buildings and rooms that are

subjected to periods of high RH, such as bathrooms and kitchens, it is necessary to use vapor retardant paint, as stated in Lstiburek's article about the "perfect wall" [21]. The use of a vapor retarder is critical in assemblies that have a portion of their thermal insulation within the vapor barrier, as in the A89F38W102 assembly for which the RH on the exterior of the fiberboard reached 64%, according to the WUFI simulation (see Figure 5d).

Moreover, how efficiently XPS acts as a vapor barrier has been studied by Smegal and al. [51]. A comparison of a poorly vapor-permeable XPS and a highly vapor-permeable mineral wool external insulation showed that they had similar RH values under normal conditions but were better able to dry in assemblies that had the highly permeable external insulation when subjected to wetting events. Using a significant amount of XPS as a vapor barrier, however, can modify the behavior of an assembly since it permits drying in both directions through the control layer. The use of XPS as a vapor barrier in cold climates is still worth studying and should be investigated in further studies, especially with varying amounts of XPS on the exterior of the assemblies.

Our results suggested that using a rigid airtight panel was beneficial for the airtightness of an assembly, whereas using a double-sealed membrane as the primary air barrier was less efficient (as observed with the A89F38W102 assembly) since the air barrier layer was not accessible during the installation of the siding and the airtightness of the connection between the siding and the wood studs could not be verified and sealed as adequately as when they were reachable. One possibility to improve the airtightness of an assembly is to use a modified bitumen membrane as an air/vapor barrier, which allows for the fastener to be sealed. The results showed that this type of membrane seemed to be more effective at sealing the fasteners that are required to attach the external cladding. However, it was less airtight than a rigid airtight panel, such as XPS. A critical point in ensuring the airtightness of a building that was constructed using an air barrier and a rigid panel assembly is the quality of the workmanship of the construction workers. A conventional assembly, such as the A140OX38 assembly, is resilient to the quality of the workmanship of the workers because multiple materials, such as high-density polyethylene fiber membranes, polyethylene membranes, OSB, XPS and gypsum, contribute to the airtightness of the assembly. Reducing the number of airtight materials that are used in an assembly increases the need for the installation of materials that are effectively airtight, especially in construction components, which is difficult to achieve. However, the results of this study suggested that it was possible to achieve an equally effective air seal by using a rigid XPS panel as the primary air sealing layer rather than a polyolefin external membrane or a polyethylene membrane.

XPS provided the best thermal performance for the A89X102 assembly. However, using XPS as the main component for thermal insulation reduces the acoustic performance of the assembly. As suggested by Berntl Zeitler et al. [32], different strategies can be used to increase the acoustic transmission loss of an assembly. From the results of this study, the assemblies that had external insulation also had added gypsum liner boards, which increased the thickness of the boards, added resilient channels and increased stud spacing. The use of 2 $\times$ 6 boards could also impact the acoustic transmittance loss but increased the overall thickness of the assembly. In addition, changing the external cladding material to a denser material, such as brick or masonry, would have a positive impact on the acoustic transmission loss of an assembly. The A140OX38 assembly was the only assembly that acted as an effective absorber since the placement of the fiberglass or mineral wool in the cavity increased the absorption coefficient by virtue of an increased damping effect.

Furthermore, the WUFI simulation results suggested that winter condensation had no impact on the humidity levels or the risk of mold growth in all of the assemblies that were studied when the exposure conditions were normal and there was either no water infiltration or a water infiltration of 0.01% from precipitation. The simulation results showed that winter condensation only impacted the sheathing or stud water content by increasing it above 30% when a water infiltration of 0.1% from precipitation was added.

Only under these conditions did the installation of all thermal insulation on the outside the structural cavity have a significant impact on the water content of the sheathing.

The choice of material that was used for the sheathing panel and the external insulation had an impact on the drying capacity of the assemblies. The hygrothermal simulation results suggested that fiberboard had a higher drying rate than OSB when subjected to high moisture contents at the beginning of the simulation since the fiberboard was more permeable than the OSB. The simulation presented a source of error, however, as the drying of the wood studs in the A89X102 assembly was measured even though the studs could not dry through the structural cavity that had no thermal insulation. This observation led to an underestimation of the assembly's drying capacity.

The simulation results suggested that climate type had little impact on the performance of the assemblies. The hygrothermal performance of the A140OX38 assembly, which had a fraction of its thermal insulation on the inside of the structural cavity, and the externally insulated assemblies was sufficient to ensure adequate moisture control within the structural cavities while providing effective thermal resistance in accordance with the QCC under normal and unfavorable exposure conditions. In fact, for the externally insulated assemblies, the exterior climate had little impact on the variations in the temperatures and relative moisture contents inside the structural layers because of the high drying rates of the assemblies. However, adding a significant amount of thermal insulation to the exterior of an assembly presents construction challenges. Particularly in a subarctic climate, the addition of significant amounts of external thermal insulation requires the connectors that support the external cladding to bear loads to a depth of more than four inches and be fastened to the wood studs. In 2013, Peter Baker of the Building Science Corporation presented several possible connection methods to ensure an adequate load carrying capacity in the presence of a large amount of external thermal insulation. The featured fasteners included Z-bars and clip and furring strip fastening systems [52]. Future research should investigate the types of fastening systems that are available in Quebec and can accommodate the installation of large amounts of insulation at an affordable price.

Finally, it is worth to recall that the hygrothermal conclusions drawn in this work are based solely on a 1D analysis of the walls and did not account for several elements such as junctions, windows, roof, floor, ventilation, etc., which could potentially increase mold growth risks in subarctic buildings.

5. Conclusions

This study presented a comparative approach that included the use of laboratory testing and hygrothermal simulations to measure the performance of various wall assemblies. The performance of externally insulated assemblies was compared to that of a modern assembly that is largely considered to be energy efficient. The comparison was based on the effective thermal resistance of the assemblies, as measured as a function of the thickness and thermal conductivity of their insulation materials. The temperature and RH profiles of the assemblies under winter conditions were measured following a 7-day conditioning period during which they were sandwiched between two climate chambers. Their airtightness was measured in the laboratory using a pressurization chamber and their ASTC index values were measured to compare the amount of sound that was transmitted through them. Hygrothermal simulations that were performed using WUFI software were used to compare the moisture contents of the intermediate sheathing panels and the risk of mold growth in cold and subarctic climates over a 2-year simulation period. The main conclusions of the project suggested that externally insulated assemblies limited the risk of condensation occurring inside the structural cavities and allowed for faster drying than that of the modern assembly in all climates that were tested when exposed to water infiltration or high water contents. The assemblies with external airtight insulation boards were more airtight than assemblies with air barrier membranes and soundproof external insulation material, such as Rockwool board, which is necessary to achieve a comparable sound transmission loss to that the modern assembly. The results also suggested the following observations:

- The modern assembly showed a dew point position inside the cavity and the highest HR out of all of the assemblies on the inside of the OSB. Condensation on the backside of the OSB was likely to occur, especially under the conditions of interior air exfiltration.
- The lower amount of insulation that was used on the exterior of the cavity in the A140OX38 assembly contributed to the temperature variations in the OSB being dependent on the temperature variations in the outside climate and led to higher RH values inside the structural cavity when subjected to cold temperatures.
- Using a rigid airtight panel was beneficial for the airtightness of an assembly, whereas using a sealed membrane as the primary air barrier layer showed higher air leakage rates.
- The apparent sound transmission class (ASTC) measurements suggested that the externally insulated assemblies performed worse than the wall assembly that had cavity insulation. Fiberboards and Rockwool boards had to be used conjointly to achieve an acoustic performance hat was comparable to that of the assembly with cavity insulation, while using extruded polystyrene as the main thermal insulation material yielded significantly lower ASTC values.
- The simulation results suggested that the moisture content and mold growth index values of the sheathing panels and wood studs remained low for all assemblies in both subarctic and cold climates when subjected to 1% rain infiltration on the backside of the external cladding and 0.1% of that rain infiltrated the external surface of the sheathing, the airflow through the assembly was 0.02 $L/s \cdot m^2$ and the initial sheathing/stud moisture content was 250 kg/m^3. The assemblies with fiberboard sheathing dried faster than the other assemblies when subjected to a high initial water content of 250 kg/m^3 and 0.1% of the rain infiltrated the external surface of the sheathing. Under these conditions, the maximum mold growth index of the fiberboard remained only slightly lower than that of the OSB or the wood studs in the other assemblies in both climates.
- The simulation results suggested that the cold and subarctic climates had little impact on the performance of the externally insulated assemblies.

Externally insulated assemblies were shown to reduce the thermal bridging that is associated with the structural elements within the structural layers of walls and using an airtight panel has been shown to have the potential to improve both thermal resistance and airtightness. The loss of mass that was caused by using 89-mm studs rather than 140-mm studs and removing insulation from the structural cavity increased the transmission of sound through the assembly, but this could be compensated for by using an absorbent porous board or insulation outside of the cavity. Over an extended period, the externally insulated assemblies dried quickly after the event of water infiltration and limited condensation periods under cold and subarctic climate conditions. Further research is needed to cover the construction details for these assemblies and to compare the simulation results from this study to experimental results.

Author Contributions: Conceptualization, A.C.-R., L.G. and P.B.; methodology, A.C.-R., L.G. and P.B.; analysis, A.C.-R.; writing—original draft preparation, A.C.-R.; writing—review and editing, A.C.-R., L.G. and P.B.; supervision, L.G. and P.B.; project administration, P.B.; funding acquisition, P.B. All authors have read and agreed to the published version of the manuscript.

Funding: This project was funded in part by the Natural Sciences and Engineering Research Council of Canada through its IRC and CRD programs (IRCPJ 461745-18 and RDCPJ 524504-18), as well as the Canada Graduate Scholarships—Master's (CGS M) program. Funding was also provided by the industrial partners of the NSERC Industrial Research Chair on Eco-responsible Wood Construction (CIRCERB).

Institutional Review Board Statement: Not applicable.

Informed Consent Statement: Not applicable.

Data Availability Statement: Some or all data, models, or code that support the findings of this study are available from the corresponding author upon reasonable request.

Acknowledgments: The authors are grateful to the Natural Sciences and Engineering Research Council of Canada for its financial support through its IRC and CRD programs (IRCPJ 461745-18 and RDCPJ 524504-18), as well as the industrial partners of the NSERC Industrial Research Chair on Eco-responsible Wood Construction (CIRCERB).

Conflicts of Interest: The authors declare no conflict of interest.

References

1. IEA. *World Energy Balances 2019*; IEA: Paris, France, 2019. Available online: https://www.iea.org/reports/world-energybalances-2019 (accessed on 19 February 2020).
2. Bilgen, S. Structure and environmental impact of global energy consumption. *Renew. Sustain. Energy Rev.* **2014**, *38*, 890–902. [CrossRef]
3. Energy Efficiency Trends in Canada. Available online: https://oee.nrcan.gc.ca/publications/statistics/trends/2016/index.cfm (accessed on 4 March 2020).
4. Québec, L. *Building Act Chapter B-1.1, Québec Official*; Québec Official Publisher: Quebec, QC, Canada, 2020.
5. National Research Council Canada. *Quebec Construction Code*; National Research Council Canada: Ottawa, ON, Canada, 2010.
6. Wu, M.H.; Ng, T.S.; Skitmore, M.R. Sustainable building envelope design by considering energy cost and occupant satisfaction. *Energy Sustain. Dev.* **2016**, *31*, 118–129. [CrossRef]
7. Dodoo, A.; Gustavsson, L.; Tettey, U.Y.A. Cost-optimized energy-efficient building envelope measures for a multi-storey residential building in a cold climate. *Energy Procedia* **2019**, *158*, 3760–3767. [CrossRef]
8. Kim, K. Optimizing Cost Effective Energy Conservation Measures for Building Envelope. *J. Assoc. Energy Eng.* **2010**, *107*, 70–80. [CrossRef]
9. Manioğlu, G.; Yilmaz, Z. Economic evaluation of the building envelope and operation period of heating system in terms of thermal comfort. *Energy Build.* **2006**, *38*, 266–272. [CrossRef]
10. Radhi, H. Can envelope codes reduce electricity and CO_2 emissions in different types of buildings in the hot climate of Bahrain. *Energy* **2009**, *34*, 205–215. [CrossRef]
11. Ürge-Vorsatz, D.; Harvey, L.D.D.; Mirasgedis, S.; Levine, M.D. Mitigating CO_2 emissions from energy use in the world's buildings. *Build. Res. Inf.* **2007**, *35*, 379–398. [CrossRef]
12. Tokbolat, S.; Nazipov, F.; Kim, J.R.; Karaca, F. Evaluation of the environmental performance of residential building envelope components. *Energies* **2019**, *13*, 174. [CrossRef]
13. Altan, H.; Mohelnikova, J.; Fric, O.; Kadlec, M. Windows and Building Envelopes, and their Influence on Indoor Thermal Comfort. In Proceedings of the 4th IASME/WSEAS International Conference on Energy & Environment (EE'09), Cambridge, UK, 24–26 February 2009; World Scientific and Engineering Academy and Society: Stevens Point, WI, USA, 2009; pp. 259–262.
14. Frenette, C.D.; Derome, D.; Beauregard, R.; Salenikovich, A. Identification of multiple criteria for the evaluation of light-frame wood wall assemblies. *J. Build. Perform. Simul.* **2008**, *1*, 221–236. [CrossRef]
15. Frenette, C.D.; Beauregard, R.; Abi-Zeid, I.; Derome, D.; Salenikovich, A. Multicriteria decision analysis applied to the design of light-frame wood wall assemblies. *J. Build. Perform. Simul.* **2010**, *3*, 33–52. [CrossRef]
16. Bomberg, M.; Onysko, D. Heat, Air and Moisture Control in the Historic Basis for Current Practices. *J. Build. Phys.* **2002**, *26*, 3–31. [CrossRef]
17. Bomberg, M.; Romanska-Zapala, A.; Yarbrough, D. Journey of American building physics: Steps leading to the current scientific revolution. *Energies* **2020**, *13*, 1027. [CrossRef]
18. Lstiburek, J.W. Two Case Studies with Failures in the Environmental Control of Buildings. *J. Therm. Insul. Build. Envel.* **1995**, *19*, 149–172. [CrossRef]
19. Straube, B.J. *Historical Development of the Building Enclosure*; Building Science Corporation: Westford, MA, USA, 2006; pp. 1–8.
20. Hutcheon, N.B. *Principles Applied to an Insulated Masonry Wall. National Research Council of Canada*; Division of Building Research: Ottawa, ON, Canada, 1964; pp. 1–7. [CrossRef]
21. Lstiburek, J.W. The Perfect Wall. *ASHRAE J.* **2007**, *49*, 74, Gale Academic OneFile. Available online: https://go.gale.com/ps/i.do?p=AONE&u=anon~adb01959&id=GALE|A165939922&v=2.1&it=r&sid=googleScholar&asid=a8313275 (accessed on 28 June 2022).
22. Lstiburek, J.W. Joseph Haydn Does The Perfect Wall. *Build. Sci.* **2015**, *57*, 64–69.
23. Straube, J.; Smegal, J. *Building America Special Research Project: High-R Walls Case Study Analysis*; Building Science Corporation: Westford, MA, USA, 2009; pp. 1–68.
24. Smegal, J.; Straube, J. *High-R Walls for the Pacific Northwest—A Hygrothermal Analysis of Various Exterior Wall Systems Hygrothermal Analysis of Various Exterior*; Building Science Corporation: Westford, MA, USA, 2010; pp. 1–91.
25. Trainor, T. The Hygrothermal Performance of Exterior Insulated Wall Systems. Master's Thesis, Master of Applied Science in Civil Engineering, University of Waterloo, Waterloo, ON, Canada, 2014.

26. Craven, C.M.; Garber-slaght, R.L. Exterior Insulation Envelope Retrofits in Sub-Arctic Environments. In Proceedings of the Seventh International Cold Climate HVAC Conference, Calgary, AB, Canada, 12–14 November 2012; pp. 1–8. [CrossRef]
27. Ge, H.; Straube, J.; Wang, L.; John, M. Field study of hygrothermal performance of highly insulated wood-frame walls under simulated air leakage. *Build. Environ.* **2019**, *160*, 106202. [CrossRef]
28. Thorburn, S. Acoustical Considerations for Mixed-Use Wood-Frame Buildings. 2014. Available online: https://www.woodworks.org/wp-content/uploads/Acoustics_Solutions_Paper.pdf (accessed on 6 June 2022).
29. Pohl, J. *Building Science: Concepts and Application*; Wiley-Blackwell: Hoboken, NJ, USA, 2011; pp. 1–271.
30. Flaherty, F.O.; Alam, M. Advances in Building Energy Research Thermal and sound insulation performance assessment of vacuum insulated composite insulation panels for building façades. *Adv. Build. Energy Res.* **2021**, *15*, 270–290. [CrossRef]
31. Soyaslan, I.I. Thermal and sound insulation properties of pumice/polyurethane composite material. *Emerg. Mater. Res.* **2020**, *9*, 859–867. [CrossRef]
32. Zeitler, B.; Hoeller, C.; Mahn, J. *Empirical Model of Direct Sound Lightweight Wood-Framed Construction Transmission through*; Inter Noise: San Francisco, CA, USA, 2015; pp. 1–9.
33. Zeitler, B.; Mahn, J.; Quirt, D.; Holler, C.; Stefan, F.; Sabourin, I. *RR-331 Guide to Calculating Airborne Sound Transmission in Buildings: Second Edition, Canada*; National Research Council Canada: Montreal, QC, Canada, 2016.
34. Connelly, M.; Stehling, E.; Tamanna, O. Measurement of the sound transmission loss of rain screen wall assemblies. In Proceedings of the 26th International Congress On Sound and Vibration, Montreal, QC, Canada, 7–11 July 2019; pp. 1–5.
35. Hukka, A.; Viitanen, H.A. A mathematical model of mould growth on wooden material. *Wood Sci. Technol.* **1999**, *33*, 475–485. [CrossRef]
36. Ojanen, T.; Viitanen, H.; Peuhkuri, R.; Lähdesmäki, K.; Vinha, J.; Salminen, K. Mold Growth Modeling of Building Structures Using Sensitivity Classes of Materials. In Proceedings of the Thermal Performance of the Exterior Envelopes of Buildings XI International Conference, Clearwater Beach, FL, USA, 5–9 December 2010; p. 18.
37. National Research Council Canada. Tables for Calculating Effective Thermal Resistance of Opaque Assemblies. 2016. Available online: https://www.nrcan.gc.ca/energy/efficiency/housing/new-homes/energy-starr-new-homes-standard/tables-calculating-effective-thermal-resistance-opaque-assemblies/14176 (accessed on 23 April 2022).
38. National Research Council Canada. *National Building Code*; National Research Council Canada: Ottawa, ON, Canada, 2010.
39. *ASTM C518-21*; Standard Test Method for Steady-State Thermal Transmission Properties by Means of the Heat Flow Meter Apparatus. ASTM International: West Conshohocken, PA, USA, 2021.
40. *ASTM E783-02*; Standard Test Method for Field Measurement of Air Leakage through Installed Exterior Windows and Doors. ASTM International: West Conshohocken, PA, USA, 2002.
41. *ASTM E336-19A*; Standard Test Method for Measurement of Airborne Sound Attenuation between Rooms in Buildings. ASTM International: West Conshohocken, PA, USA, 2019.
42. *ASTM E413-16*; Classification for Rating Sound Insulation. ASTM International: West Conshohocken, PA, USA, 2016.
43. ASHRAE. *Addendum e to ANSI/ASHRAE Standard 160-2009*; Criteria for Moisture-Control Design Analysis in Buildings. American Society of Heating, Refrigerating and Air-Conditioning Engineers, Inc. (ASHRAE): Atlanta, GA, USA, 2016.
44. Glass, S.V.; Gatland, S.D.; Ueno, K.; Schumacher, C.J. Analysis of Improved Criteria for Mold Growth in ASHRAE Standard 160 by Comparison with Field Observations. In *Advances in Hygrothermal Performance of Building Envelopes: Materials, Systems and Simulations*; Mukhopadhyaya, P., Fisler, D., Eds.; ASTM International: West Conshohocken, PA, USA, 2017; pp. 1–27.
45. Lstiburek, J.W. Insight WUFI: Barking up the wrong tree? *ASHRAE J.* **2015**, *57*, 62–70. [CrossRef]
46. Straube, J.F.; Burnett, E.; VanStraaten, R.; Schumacher, C. *Ventilated Wall System: Review of Literature and Theory. Building Engineering Group report for ASHRAE Research Project 1091—Development of Design Strategies for Rainscreen and Sheathing Membrane Performance in Wood Frame Walls*; American Society of Heating, Refrigerating and Air-Conditioning Engineers, Inc. (ASHRAE): Atlanta, GA, USA, 2004; Available online: https://www.techstreet.com/ashrae/standards/rp-1091-development-of-design-strategies-for-rainscreen-and-sheathing-membrane-performance-in-wood-frame-walls?gateway_code=ashrae&product_id=1719090#product (accessed on 18 December 2021).
47. Rouleau, J.; Gosselin, L.; Blanchet, P. Understanding energy consumption in high-performance social housing buildings: A case study from Canada. *Energy* **2018**, *145*, 677–690. [CrossRef]
48. Holm, A.; Glass, S.; Antretter, F. Interior Temperature and Relative Humidity Distributions in Mixed-Humid and Cold Climates as Building Simulation. In Proceedings of the Thermal Performance of the Exterior Envelopes of Whole Buildings—11th International Conference, Clearwater Beach, FL, USA, 5–9 December 2010; pp. 1–11.
49. Arena, L.; Mantha, P. *Moisture Research—Optimizing Wall Assemblies*; National Renewable Energy Lab. (NREL): Golden, CO, USA, 2013.
50. Hun, D.E.; Spafford, P.; Desjarlais, A.O. *Evaluation of Air Barriers for Residential Buildings*; ORNL/TM-2013/604; Oak Ridge National Laboratory: Oak Ridge, TN, USA, 2014; pp. 1–57.
51. Smegal, J.; Finch, G.; Nieto, A.; Schumacher, C. Comparing the enclosure wall performance of low-permeance exterior insulation to high-permeance exterior insulation in the Pacific Northwest. *ASTM Spec. Tech. Publ.* **2017**, *1599*, 95–121. [CrossRef]
52. Baker, P. *Expert Meeting Report: Cladding Attachment over Exterior Insulation*; National Renewable Energy Lab. (NREL): Golden, CO, USA, 2013; pp. 1–64.